PEROVSKITE OXIDES: OXYGEN ELECTROCATALYSIS AND BULK STRUCTURE

R.E. Carbonio‡, C. Fierro, D. Tryk, D. Scherson, and E. Yeager
Case Western Reserve University
Cleveland, Ohio 44106

Perovskite-type oxides have been considered for use as oxygen reduction and generation electrocatalysts in alkaline electrolytes . This paper is concerned with perovskite stability and electrocatalytic activity, and the possible relationships of the latter with the bulk-solid state properties.

Perovskite oxides have not been found in general to be very active for oxygen reduction, although substantial catalytic activity for hydrogen peroxide decomposition has been found. Instability of some perovkites has been observed over particular potential ranges. In some cases these ranges overlap those in which O_2 reduction occurs.

A series of compounds of the type $LaFe_xNi_{1-x}O_3$ has been used as a model system to gain information on the possible relationships between surface catalytic activity and bulk structure. Hydrogen peroxide decomposition rate constants have been measured for these compounds. **Ex-situ** Mossbauer effect spectroscopy (MES), and magnetic susceptibility measurements have been used to study the solid state properties. X-ray photoelectron spectroscopy (XPS) has been used to examine the surface. MES has indicated the presence of a paramagnetic-to magnetically ordered phase transition for values of x between 0.4 and 0.5. For $0 < x \leq 0.4$ the compounds are paramagnetic, as indicated by the absence of a Zeeman effect in the MES spectra. For $0.5 \leq x \leq 1.0$ the observed Zeeman effect in the MES spectra indicates the presence of a magnetically ordered phase. Complementary magnetic susceptibility measurements indicate that the compounds are antiferromagnetically ordered.

MES also shows that the introduction of Ni into the Fe(III) matrix of $LaFeO_3$ forces some of the Fe(III) into the unusual Fe(IV) state, while part of the Ni(III) is changed to Ni(II), as indicated by XPS.

The hydrogen peroxide decomposition rates have been found to undergo a substantial change in the range $0.25 < x < 0.5$. A correlation has been found between the values of the MES isomer shift and the catalytic activity for peroxide decomposition. Thus, the catalytic activity can be correlated to the d-electron density for the transition metal cations.

INTRODUCTION

Perovskite-type oxides constitute a family of oxides of the type ABO_3, with structures similar to that of the mineral perovskite $CaTiO_3$ (1, 2). Depending on the nature of the A and B cations, the chemical and physical properties can vary over a wide range. An attractive feature is that these

‡ INFIQC, Depto. de Fisico Quimica, Fac. de Ciencias Quimicas, Univ. Nac. de Cordoba. Cordoba. Argentina.

properties can be varied by preparing materials of the type $A_xA'_{1-x}B_yB'_{1-y}O_3$. Their electronic conductivity can vary from insulating to metallic conducting and even superconducting. The magnetic properties can vary from paramagnetic to ferro- or antiferromagnetic. Such compounds are very interesting both from the catalytic and the bulk properties points of view. Mixed oxidation states of both A and B cations are involved. Even if A is not catalytically or electrochemically active, it is possible to control the oxidation state of B by changing the relative amount and nature of the A cation. These materials have been synthesized and studied by several authors (3-6). The objective of this paper is to examine the relationship of the electrochemical properties of these perovskites to their bulk structures.

Since the work of Meadowcroft (7), many workers have examined O_2 reduction and generation on perovskites (8-17). In the more applied work, good performance and stability in long-term operation have been observed for O_2 generation (8, 13). For O_2 reduction, however, good performance is typically observed in short-term operation, but the performance often degrades with time (12).

Matsumoto et al. (8) have examined O_2 generation and reduction on perovskite-type oxides. They were the first to study $LaNiO_3$ as an electrode material for O_2 reduction (8). They used X-ray diffraction to analyze changes in the structure due to exposure to the electrolyte at various potentials. Karlsson (11, 12) has reported that under prolonged cathodic polarization in alkaline solution, $LaNiO_3$ reduces irreversibly to $Ni(OH)_2$ and $La(OH)_3$, thus leading to a gradual loss of performance for O_2 reduction.

Bockris and Otagawa (13, 14) have examined O_2 generation on $LaNiO_3$ as well as a number of other perovskites. They used X-ray photoelectron spectroscopy (XPS) to analyze the surface composition of these perovskites before and after exposure to the electrolyte and proposed that some of the surfaces were different in composition from that of the nominal bulk stoichiometry. The results however should be treated with caution, since it is difficult to use XPS for the quantitative surface analysis of oxides.

Recently in the authors' laboratory (13), it has been shown using Mossbauer effect spectroscopy (MES) that $SrFeO_3$ undergoes an irreversible reduction to $Fe(OH)_2$ in alkaline solution when the potential is set more negative than ca. -0.7 V vs. Hg/HgO, OH^-. These examples point to the possibility that the surface and even the bulk structure of the perovskite can be modified, even irreversibly, under certain potential conditions.

There have been several attempts to relate surface and bulk properties of the perovskites with both O_2 reduction and generation (8, 13, 14). Matsumoto and coworkers (8) have proposed correlations of catalytic activity with the existence of a σ^* band. Bockris and Otagawa (13, 14) have proposed that the catalytic activity for O_2 generation of transition metal-containing perovskites is correlated with the occupancy of the antibonding orbitals of a hydroxylated surface transition metal cation. A variety of bulk physical properties were examined and found not to correlate with the catalytic activity.

While generally speaking it is not valid to correlate bulk properties

with catalytic activity, in selected instances a bulk property can produce an effect upon the surface properties and thus upon the catalysis. In the present work compounds of the type $LaFe_xNi_{1-x}O_3$ have been examined using MES and magnetic susceptibility, which are bulk characterization techniques, and XPS, which is a surface or near-surface (ca. 1-2 nm) technique. A correlation has been found between the catalytic activity for peroxide decomposition and the MES isomer shift.

EXPERIMENTAL

Four preparative methods have been used, the solid state reaction (SSR), nitrate decomposition (ND) and precipitation methods, the latter including the hydroxide precipitation (HP) and inorganic complex precipitation (ICP) methods. In the SSR method a mixture of the oxides of the component elements is ground and then heated at a controlled temperature between 900 and 1100° C. In the ND method (18) a concentrated solution of citric acid is added to a concentrated solution of the metal nitrates so that the molar ratio of citric acid to total metal was 1. The solution was evaporated in a rotary evaporator at 40° C until the precipitate acquired the consistency of a viscous syrup. The residual water was evaporated in a vacuum oven at 110° C for 24 hours. The precursor thus obtained is a fine mixture of the nitrates and citric acid. After being burned at ~200° C, the precursor, which is then black in color, is heated at 900° C in air for 24 hours.

In the HP method a concentrated solution of an organic base (e. g., methylamine) is added to a solution of the metal nitrates. The precipitate is filtered and dried at 110° C in a vaccum oven and then heated in air at a temperature between 600 and 750° C for 24 hours.

In the ICP method a solution of the A ion nitrate [e.g., $La(NO_3)_3$] is added to a solution of a soluble form of the inorganic complex [e.g., $K_3Fe(CN)_6$] and a precipitate of the complex substituted with the A ion is obtained [e.g., $LaFe(CN)_6$]. The precipitate is filtered, dried in a vaccum oven at 110° C for 24 hours and then heated in air at a temperature between 450 and 700° C for 24 hours. Usually the ICP method requires only a very low temperature for the synthesis because of the molecular level mixing of the A and B ions.

Some of the compounds have been examined using X-ray diffraction and found to exhibit no detectable phase impurities. The rest are in progress and the results will be presented in a more detailed report.

XPS measurements were done with a Varian IEE-15 X-ray photoelectron spectrometer equipped with a high-intensity magnesium anode (K_α radiation, 1253.6 eV). The operating parameters were: X-ray power, 640 W (8 kV, 80 mA), analyzer energy, 100 kV, channel width, 0.18 eV. The analyzer pressure was 10^{-6}-10^{-7} torr. An internal standard of Au powder was used in an intimate mixture with the sample to correct for energy shifts caused by surface charging.

The Mossbauer spectra were recorded with a Ranger Scientific MS-900 system, and the statistical analysis performed with the STONE routine (19). The Mossbauer parameters are reported vs. α-iron.

The magnetic susceptibility measurements were performed with a Faraday electrobalance (Cahn RG) with a magnetic field of ~ 10 kG. Ni(ethylenediamine)$_3S_2O_3$ and $Hg[Co(SCN)_4]K_6$ were used as standards for calibration.

For the electrode preparation equal amounts of the catalyst and Shawinigan Black (SB, Gulf Oil Chemicals) (an acetylene black with an approximate surface area of 65 m^2/g) were mixed in water under ultrasonic agitation. A dilute Teflon emulsion (T30B, Dupont) was added to the mixture such that 25 wt.% of the total weight was Teflon. The mixture was then filtered through a fine pore membrane (Nucleopore, polycarbonate membrane, 1.0 μm). The resulting carbon/perovskite/Teflon paste was kneaded until rubbery and then placed on top of a disk of electronically conductive hydrophobic material (Electromedia Corp. Englewood, NJ) containing a nickel screen or carbon fiber in a 1.75 cm diameter die and pressed at 340 kg cm^{-2}. The electrode disk was then trimmed to obtain a rectangle 0.5 x 1.0 cm. A nickel screen was used as the counter electrode and the reference electrode was Hg/HgO, OH^-. The electrochemical experiments were performed either in 0.1 M or 4 M KOH at room temperature.

Hydrogen peroxide decomposition measurements were performed at 22° C using the gasometric method. A small amount of the catalyst (~ 10 to 50 mg) was dispersed in 50 cm^3 of 4 M KOH prepared from distilled water and KOH pellets (Fisher Scientific, Reagent Grade). The initial concentration of HO_2^- was 0.2 M.

RESULTS

A. Bulk Structure

The MES spectra for the different perovskite compositions are shown in Fig. 1. These show for $0 < x \leq 0.4$ the presence of two peaks, which can be attributed formally to Fe^{3+} and Fe^{4+} sites. The existence of Fe^{4+} in perovskites has been reported before for $SrFeO_3$ (4, 20), although in the present case the isomer shift apparently is not as negative as it is in the case of Fe^{4+} in $SrFeO_3$. The site with the less positive isomer shift will be provisionaly assigned to Fe^{4+}. The absence of a six-line splitting in the spectra provides evidence that in the $0 < x \leq 0.4$ compositional region the perovskite is paramagnetic. For $0.5 \leq x \leq 1.0$, however, the spectra yielded six lines, characteristic of a magnetically ordered species. A singlet is also observed, which shows that a paramagnetic phase is still present. This could be explained as follows: statistically, there should be two types of iron atoms for intermediate compositions (i.e. when x ~ 0.5). One type of iron will be mainly surrounded by nickel atoms, and this will lead to the formation of a "paramagnetic site", which will have Fe preferentially in the formal 4+ state. Another type will be surrounded by iron atoms, leading to the formation of an "antiferromagnetic site", which will have Fe preferentially in the 3+ state. The six-line spectra at $x \geq 0.5$ can be attributed to Fe^{3+} and the singlet to Fe^{4+}. This can be supported by the continuity of the isomer shift vs. x curve (Fig. 2), for both types of sites. Two types of iron sites have been observed for $LaFe_xRu_{1-x}O_3$ with MES by Bouchard et al.(3). In that case however both were in the +3 state and were also paramagnetic. Another possible explanation is the existence of two distinct phases for intermediate compositions, one paramagnetic and the other antiferromagnetic, each one with a given isomer

shift which remains relatively constant. The possible existence of two phases must be checked using X-ray diffraction measurements.

A plot of the isomer shift vs. x indicates that the difference in isomer shift between the two types of sites (or phases) reaches a maximum at x = 0.25. Only one type of site (or phase) is present at the two extremes. The composition with x ~ 0 has been assigned using the compound $LaFe_{0.0013}Ni_{0.9987}O_3$, in which all of the iron is ^{57}Fe in order to obtain a good MES signal. Since the isomer shift is a direct measurement of the electron density surrounding the nucleus, it can be concluded that there is a maximum in the difference between the electron densities for the Fe^{3+} and Fe^{4+} sites (or phases) at 25% of iron.

Mossbauer effect spectroscopy has shown that in $LaFe_xNi_{1-x}O_3$, depending on x, Fe is in two oxidation states (i.e. 3+ and 4+). It is interesting to analyze the oxidation states of Ni in the same structure. It is supposed then that, in order to maintain electroneutrality, Ni must be in the 2+ state. (In pure $LaNiO_3$ the normal oxidation state is 3+.) XPS is suitable for checking this possibility if the caveat already mentioned in the introduction is kept in mind.

The $2p_{3/2}$ Ni bands for $LaFe_xNi_{1-x}O_3$ perovskites for different values of x are shown in Fig. 3. One peak is at binding energies between 853 and 855 eV (depending on the composition). As the amount of iron increases, a new peak starts to develop at lower energies, and the original peak is shifted towards higher energies. This is possibly due to a change from good

electronic conduction for low Fe content to semiconducting properties for high Fe content, which will change the surface energy with respect to the Fermi level in the bulk of the semiconductor. At 90 mol% iron, two clearly defined peaks are observed, with the one at lower energies attributed to a Ni^{2+} species. These results are consistent with those obtained from Mossbauer spectroscopy. When Ni is introduced in $LaFeO_3$, part of the original Fe^{3+} is oxidized to Fe^{4+}, and the Ni valence is distributed between the 2+ and 3+ states, so that the formula of the compound can be writen as $LaFe(III)_xFe(IV)_{1-x}Ni(III)_yNi(II)_{1-y}O_3$, where the x and y values depend upon the overall composition. The appearance of Fe^{4+} ions when Ni^{2+} is oxidized to Ni^{3+} has been observed by Corrigan et al.(21) in battery-type nickel hydroxide electrodes doped with iron hydroxide using Mossbauer spectroscopy.

The combination of oxidation sates of B and B' in $LaB_xB'_{1-x}O_3$ regulates the total magnetism of the compound. Thus Fe^{3+} is in a high spin state ($t_{2g}^3\ e_g^2$) in $LaFeO_3$ (22), and this compound is antiferromagnetically ordered. Ni^{3+} is in a low spin state ($t_{2g}^6\ e_g^1$) in $LaNiO_3$ (22), and the compound is a Pauli paramagnet. As was previously mentioned there is a transition from a paramagnetic to a magnetically ordered state in the $0.4 < x < 0.5$ region. The specific assignment of antiferromagnetism for the compounds in the range $x \geq 0.5$ is supported by magnetic susceptibility measurements. The gram magnetic susceptibilities (χ_g) at room temperature are shown in Table I as a function of x. The values of χ_g are to small to be assigned to the ferromagnetic state, for which χ_g should be on the order of 10^{-2}-10^4 emu g^{-1} (23). The χ_g values for paramagnetic or antiferromagnetic compounds should be in the range 0-10^{-4} emu g^{-1}. For these reasons the compounds with $x > 0.5$ are antiferromagnetic, as is $LaFeO_3$ (24).

Perovskites of the type $LaB_xB'_{1-x}O_3$ offer the opportunity to change the distribution of the oxidation states, which can be very useful from the point of view of catalysis. The solid state properties can be changed more or less continuously with composition. For this reason the series of $LaFe_xNi_{1-x}O_3$ perovskites has been chosen as a model system for the examination of electrochemical and catalytic properties.

B. Electrochemical Stability

The voltammograms for $LaFeO_3$ and $LaFe_{0.75}Ni_{0.25}O_3$ are shown in Fig. 4. The electrodes were prepared in the form of a thin porous coating, as described in the experimental section. Over a wide potential range $LaFeO_3$ exhibits no voltammetric peaks. This is consistent with the fact that $LaFeO_3$ is an insulator(1, 22, 24). The introduction of Ni into the $LaFeO_3$ structure increases its conductivity (25), and for $x < 0.2$ the compound is a metallic conductor. As shown in Fig. 4b, the introduction of 25 mol% Ni in $LaFeO_3$ makes it sufficiently conducting to observe redox peaks. Two redox couples are present, one centered at ca. -0.5 V, corresponding to the Fe(III)/Fe(II) couple and the other centered at ca. +0.52 V, corresponding to the Ni(III)/Ni(II) couple. The shapes and positions of the peaks are similar to those for the respective hydrated oxides [$FeOOH/Fe(OH)_2$ and $NiOOH/Ni(OH)_2$] (26). The peak separation for the Fe(III)/Fe(II) redox couple is exaggerated in this case however. A shift in the nickel peaks due to the presence of iron is also observed in this case, as is observed in the Fe/Ni oxyhydroxides(26, 27).

As judged by the integrated charge associated with the voltammetric peaks in the case of $LaFe_{0.75}Ni_{0.25}O_3$ (Fig. 4b), only the surface is involved in the redox processes. (The surface areas of these perovskites are on the order of 1 to 3 m^2/g.) In order to gain additional information concerning the redox processes, in-situ MES was performed with $LaFe_{0.25}Ni_{0.75}O_3$ in 4 M KOH. The ex-situ MES spectrum of the dry electrode and the in-situ MES spectra after polarization at +0.5 , 0.0 and -1.2 V vs. Hg/HgO, OH^- (not shown) are all almost the same. This is consistent with the previously mentioned finding that only a small fraction of the material was involved in the redox process (~ 2 % of the total), which corresponds to material in a thin surface layer.

Since all of the iron in $SrFeO_3$ should be in the 4+ state, it has been used in electrochemical, MES and XPS experiments to provide a reference, even though it is known that the compound is not completely stoichiometric except under special conditions. It is a metallic conductor so that no problems arose due to poor electronic conductivity. The results obtained with cyclic voltammetry are shown in Fig. 5. The anodic and cathodic potential limits were increased in steps. No faradaic current was observed between -0.5 and +0.6 V (Fig. 5a). At +0.6 V anodic current due to O_2 generation was observed. At potentials more negative than -0.5 V, a cathodic peak was observed with a complementary anodic peak in the positive sweep. A voltammogram between the limits -1.3 V and +0.8 V is shown in Fig. 5b. The Fe(III)/Fe(II) redox couple is observed, as in the case of $LaFe_{0.75}Ni_{0.25}O_3$. In this case, however, ca. 100 % of the material takes part in the redox process. In-situ MES performed in this laboratory (28) have shown that $SrFeO_3$ is irreversibly reduced to $Fe(OH)_2$ at potentials more negative than ca. -0.7 V vs. Hg/HgO, OH^- and that, under subsequent anodic polarization at -0.3 V, FeOOH is obtained.

C. Catalytic Activity

In order to examine possible relationships between catalytic activity and bulk structure, the hydrogen peroxide decomposition reaction has been chosen due to its important role in oxygen electrochemistry. Hydrogen peroxide decomposition rate constants have been measured for the $LaFe_xNi_{1-x}O_3$ series using the gasometric method. The rate constants are plotted in Fig. 6 as a function of x. These results should be treated with some caution, however, since they are not normalized to the surface areas.

A maximum is observed at 25% Fe content. This correlates very approximately with the isomer shift variations for Fe^{3+} and Fe^{4+} noted above. The range of x values for which the difference in the electron density for both sites is at a maximum corresponds to that for which the maximum activity for hydrogen peroxide decomposition is observed. It is possible that both the mixed oxidation state for Fe and/or Ni and the unusual presence of Fe^{4+} sites may be factors in promoting the catalytic activity.

This correlation could be considered reasonable in the light of the traditional explanation of hydrogen peroxide decomposition catalysis as proposed by Latimer (29). Any redox couple which falls in the potential range between the O_2/HO_2^- and HO_2^-/OH^- couples can in principle catalyze the disproportionation reaction. If a catalyst simultaneously contains both strongly oxidating and strongly reducing species, the coupled HO_2^- oxidation and reduction might be fast.

REFERENCES

1) Voorhoeve, R. J. H. in "Advanced Materials in Catalysis", Burton, J. J. and Garten, R. L., Eds., Academic Press, New York, 1977, p. 129.

2) Voorhoeve, R. J. H.; Johnson, D. W., Jr.; Remeika, J. P. and Gallagher, P. K.; Science, **195**, 4281 (1977).

3) Bouchard, R. J.; Wehier, J. F. and Gillson, J. L.; J. Solid State Chem., **21**, 135 (1977).

4) Shimony, U. and Knudsen, J. M.; Phys. Rev., **144**, 361 (1966).

5) Obayashi, H.; Kudo, T. and Gejo, T.; Jap. J. Appl. Phys., **13**, 1 (1974).

6) Gibb, T. C.; Greatrex, R.; Greenwood, N. N. and Snowdon, K. G.; J. Solid State Chem., **14**, 193 (1975).

7) Meadowcroft, D. B.; Nature **226**, 847 (1970).

8) Tamura, H.; Yoneyama, H.; and Matsumoto, Y. in "Electrodes of Conductive Metallic Oxides". Elsevier, New York, Amsterdam. (1980-1981). Trasatti, S., Ed.

9) Kobussen, A. G. C.; Van Buren, F. R.; Van Den Belt, T. G. M. and Van Wees, H. J. A.; J. Electroanal. Chem., **96**, 123 (1979).

10) Kobussen, A. G. C.; Willems, H. and Broers, G. H. J.; J. Electroanal. Chem., **142**, 67 (1982).

11) Karlsson, G.; Electrochim. Acta, **30**, 1555 (1985).

12) Karlsson, G.; J. Power Sources, **10**, 319 (1983).

13) Bockris, J. O'M. and Otagawa, T.; J. Electrochem. Soc., **131**, 290, (1983).

14) Bockris, J. O'M.; Otagawa, T. and Young, V.; J. Electroanal. Chem., **150**, 633 (1983).

15) Tseung, A. C. C.; J. Electrochem. Soc., **125**, 1660 (1978).

16) Kudo, T.; Obayashi, H. and Yoshida, M.; J. Electrochem. Soc., **124**, 321 (1977)

17) Calvo, E. J.; Drennan, J.; Kilver, J. A.; Albery, W. J. and Steele, B. C. H.; in McIntyre, J. D. E.; Weaver, M. J. and Yeager, E. B. (Eds.), "The Chemistry and Physics of Electrocatalysis"; The Electrochemical Society, N. J., (1984), pp 489.

18) Tascon, J. M. D.; Mendioroz, S. and Gonzalea Tejuca, L.; Z. Fhys. Chem. N. F., **124 S**, 109 (1981).

19) Dr. M. Darby Dyar from the University of Oregon make available the statistical analysis routine.

20) Shirane, G.; Cox, D. E. and Ruby, S. L.; Phys. Rev., **125**, 1158 (1962).

21) Corrigan, D. A.; Fierro, C. and Scherson D. (to be published).

22) Goodenough, J. B.; in Reiss, H., Ed. "Progress in Solid State Chemistry", Vol. 5. Pergamon Press. Oxford, (1971). pp. 313.

23) Figgis, B. N. and Lewis, J.; in Techniques of Inorg. Chem., Vol. IV, 1965, pp. 137-248. Jonassen, H. B. and Weissberger, A. (Eds.), Wiley-Interscience, New York.

24) Goodenough, J. B. and Longo, J. M.; "Crystallographic and Magnetic Properties of Perovskite and Perovskite Related Compounds", Landolt-Bornstein Tabellen, Neue Serie III/4a, Springer-Verlag, Berlin. (1970).

25) Rao, C. N. R.; Parkash, Om and Ganguly, P.; J. Solid State Chem., **15**, 186 (1975).

26) Cordoba, S. I.; Carbonio, R. E.; Lopez Teijelo, M. and Macagno, V. A., Electrochim. Acta, **10**, 1321 (1986).

27) Corrigan, D. A.; J. Electrochem. Soc., **134**, 377 (1987).

28) C. Fierro, R. E. Carbonio, D. Scherson and E. Yeager. 171st Meeting of the Electrochem. Soc.; Philadelphia. Pennsylvania. May 1987.

29) Latimer, W. M.; Oxidation States of the Elements and their Potentials in Aqueous Solutions, 2nd Edn., Prentice Hall, New Jersey, 1952, p. 44.

TABLE I

Compound	χ_g 10^6/(emu g^{-1})
$LaNiO_3$	5.2
$LaFe_{0.1}Ni_{0.9}O_3$	24.3
$LaFe_{0.25}Ni_{0.75}O_3$	12.6
$LaFe_{0.50}Ni_{0.50}O_3$	15.4
$LaFe_{0.75}Ni_{0.25}O_3$	12.4
$LaFe_{0.90}Ni_{0.10}O_3$	13.2
$LaFeO_3$	9.9

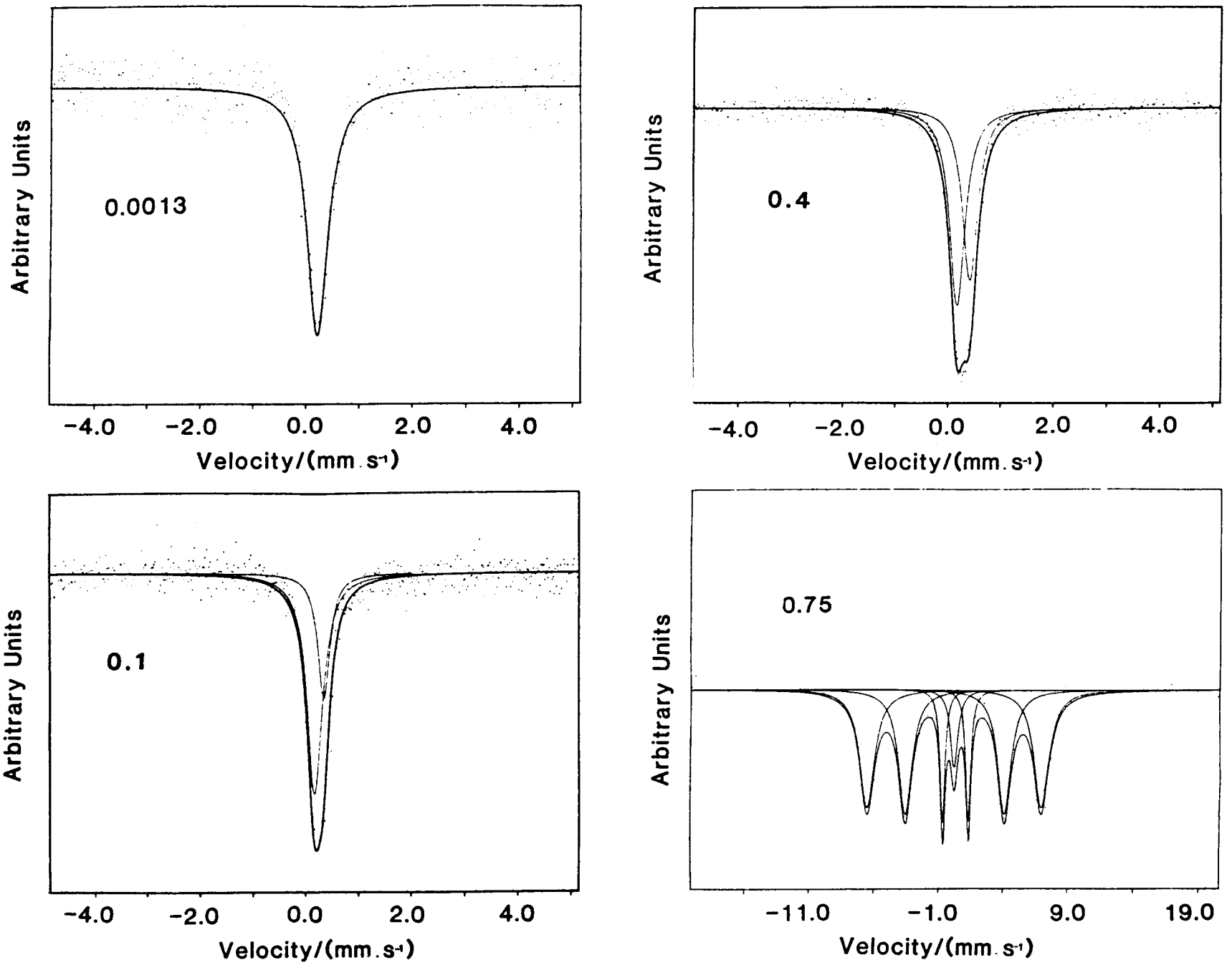

Figure 1: Ex-situ MES for $LaFe_xNi_{1-x}O_3$ for different values of x (the values of x are indicated in the figures).

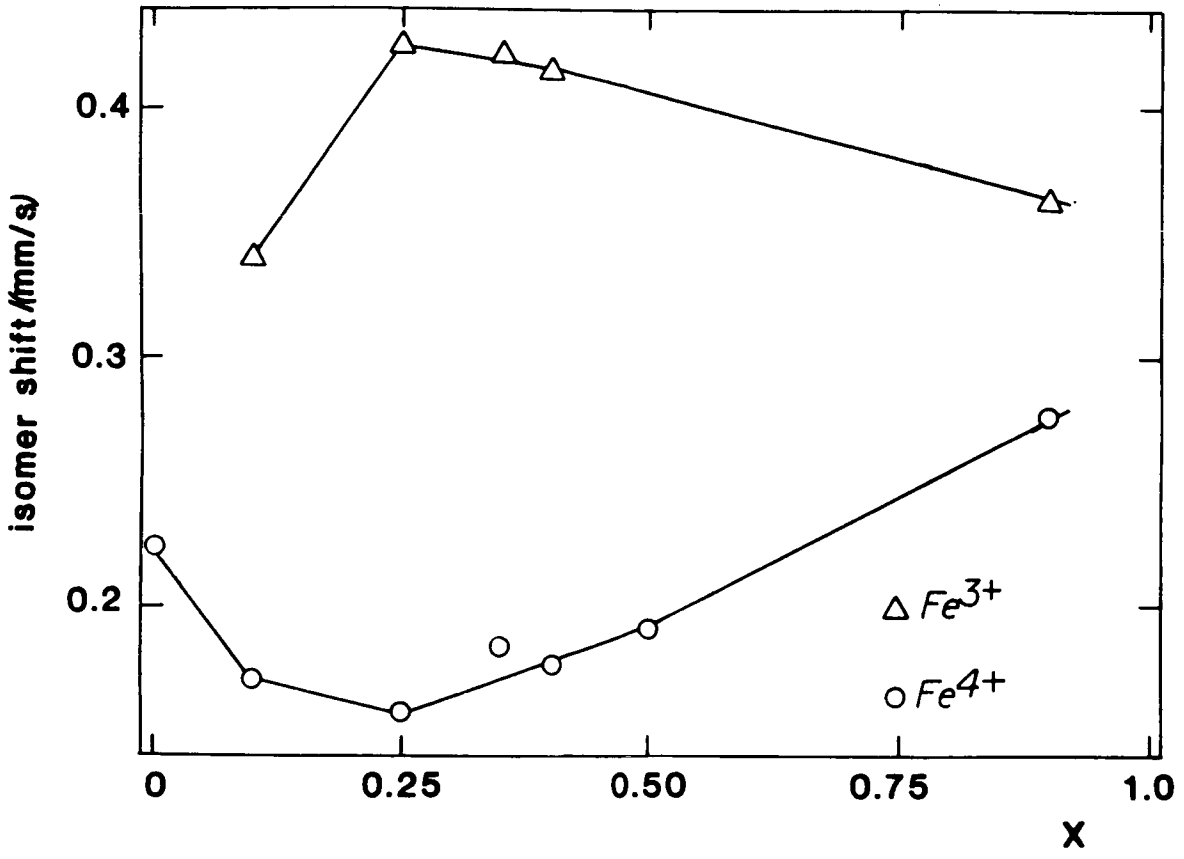

Figure 2: Isomer shift (δ) of Fe^{3+} (δ_1) and Fe^{4+} (δ_2) for $LaFe_xNi_{1-x}O_3$ as a function of x.

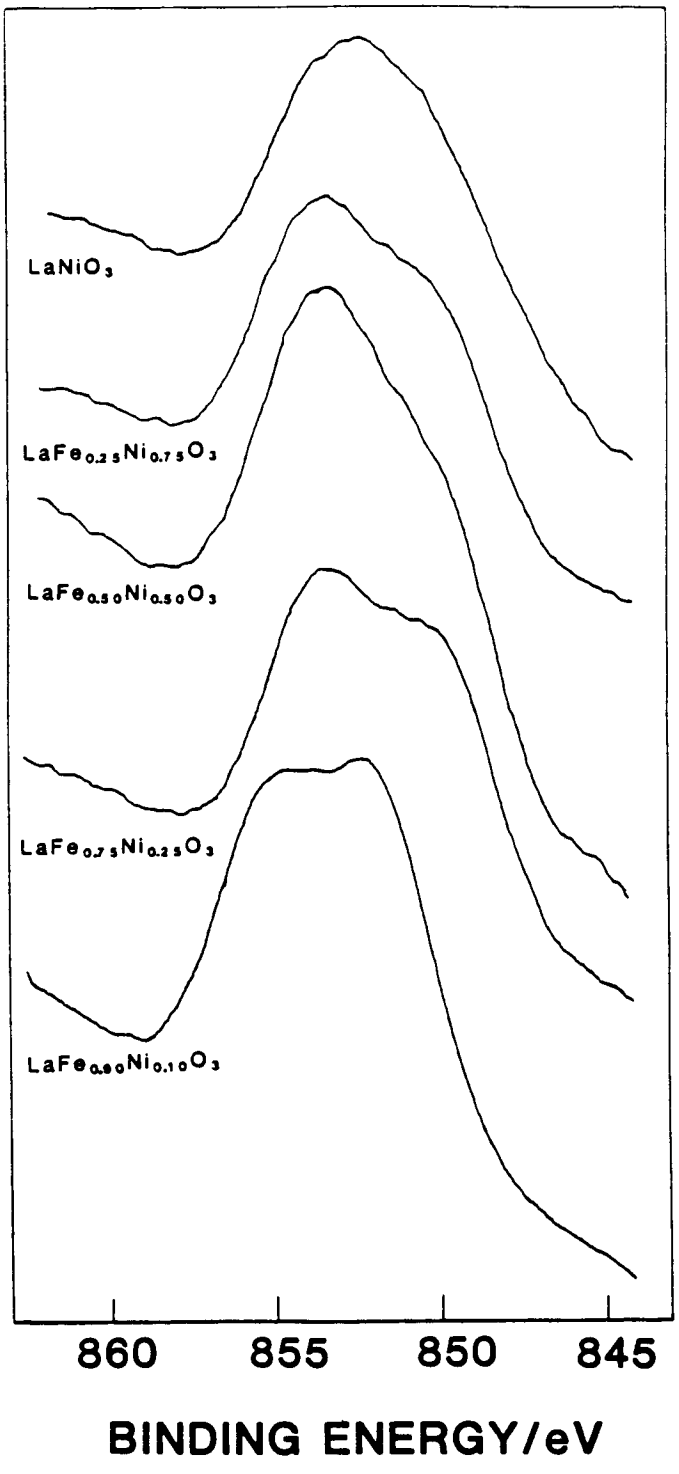

Figure 3: X-ray photoelectron spectra of the Ni $2p^{3/2}$ bands of $LaFe_xNi_{1-x}O_3$ for different values of x.

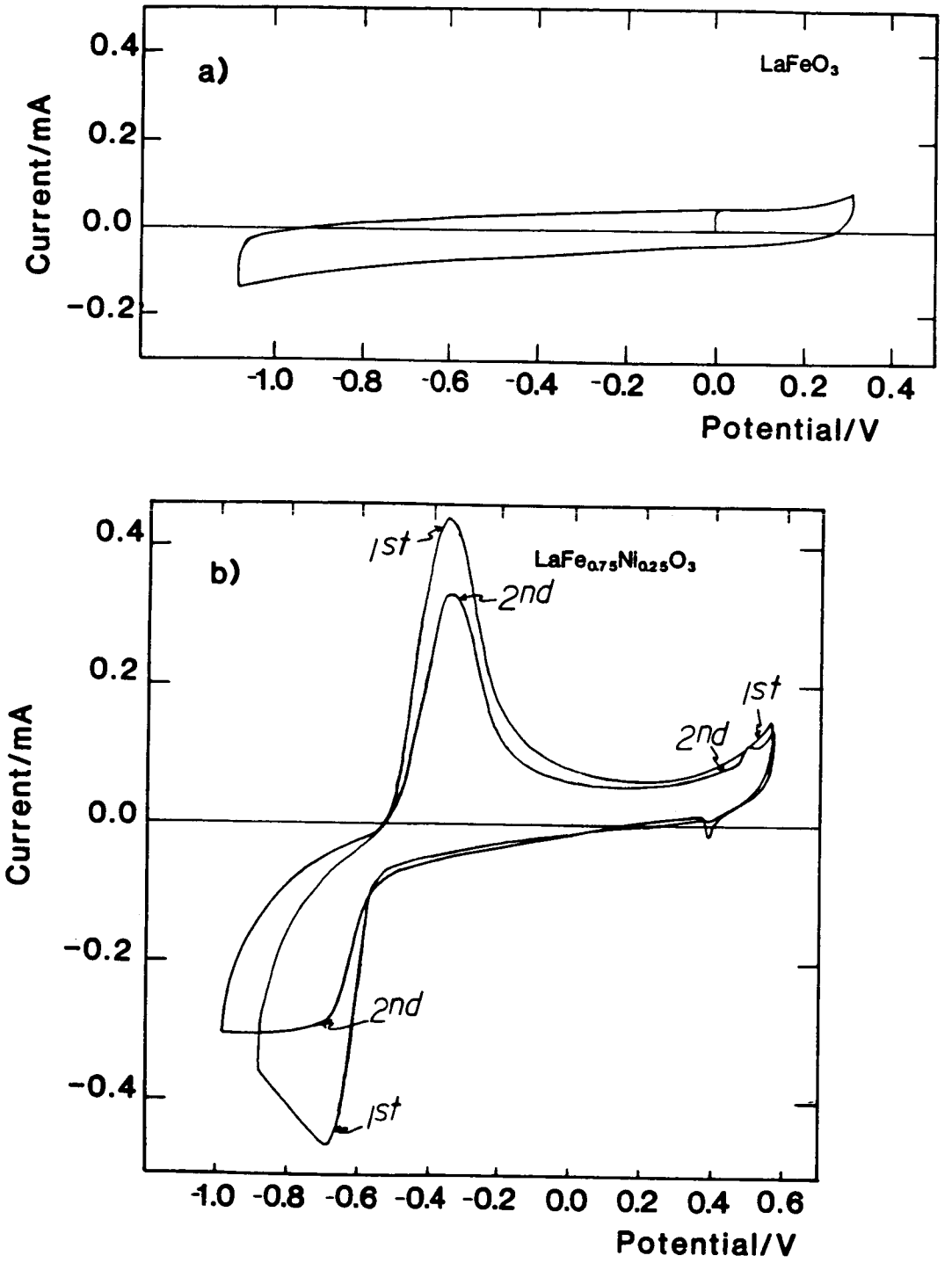

Figure 4: Cyclic voltammograms for thin porous coating electrodes of 50% perovskite in SB carbon on a pyrolytic graphite disk. Electrolyte: 0.1 M KOH, N_2 saturated. Scan rate: 10 mV/s.

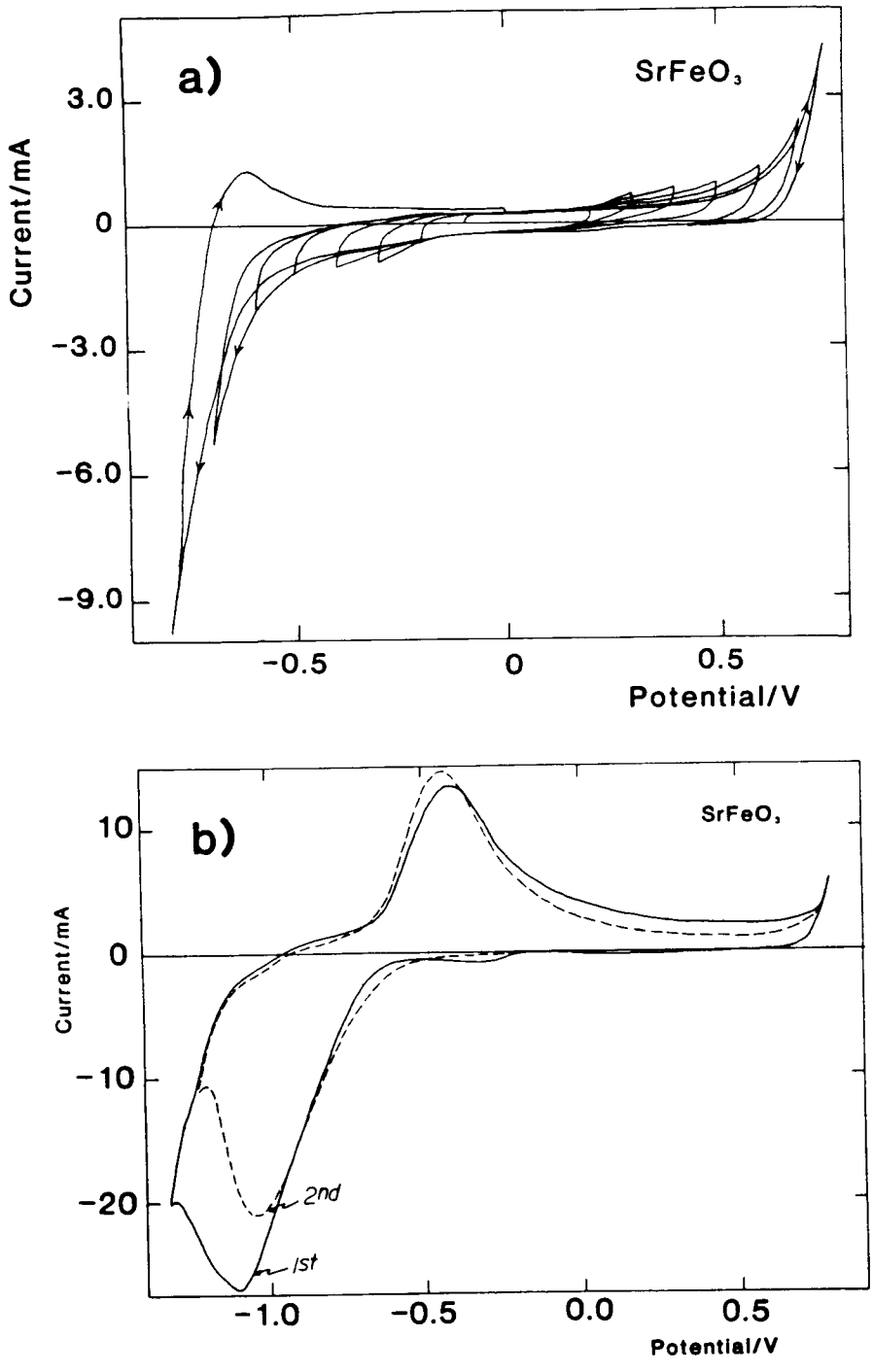

Figure 5: Cyclic voltammograms for floating gas-fed electrodes containing 15 mg cm^{-2} of $SrFeO_3$ plus 15 mg cm^{-2} of SB carbon. Electrolyte: 0.1 M KOH, N_2 saturated. Scan rate: 10 mV/s.

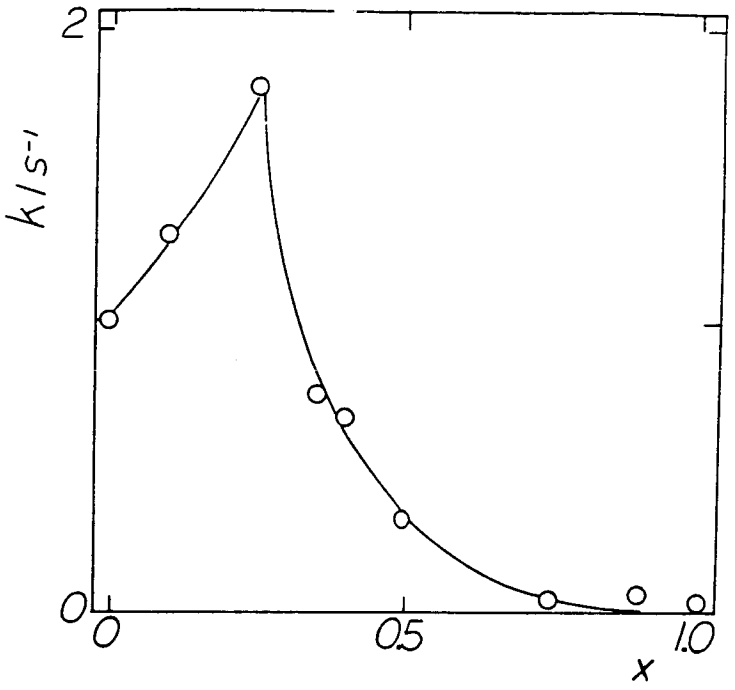

Figure 6: Hydrogen peroxide decomposition rate constants vs. x in $LaFe_xNi_{1-x}O_3$.
The rate constants were measured by the gasometric method in 4 M KOH at 22° C. The initial concentration of peroxide was 0.2 M.